CHIN. PHYS. LETT. Vol. 36, No. 3 (2019) 034303

Dynamic Superposition and Levitation Capability of Two Confronting Ultrasonic Waves *

Na Yan(闫娜), Wen-Li Di(邸文丽), Zhen-Yu Hong(洪振宇), Wen-Jun Xie(解文军), Bing-Bo Wei(魏炳波)**
Department of Applied Physics, Northwestern Polytechnical University, Xi'an 710072

(Received 29 December 2018)

The superposition dynamics of two confronting ultrasonic waves and their levitation capability for centimeter-sized thin disks are investigated by numerical analyses and validated by experiments. The sound pressure simulation reveals that two opposite ultrasonic waves provide a more effective standing-wave field than a single ultrasonic wave when the diameter of disk-shaped object approaches the wavelength scale. The dynamic superposition of two confronting beams facilitates the acoustic levitation of the clay disk and aluminum disk with diameters of 0.97λ and 0.90λ. The acoustic radiation forces exerting on these thin disks are measured experimentally, which exhibit a better levitation stability for the centimeter-sized thin disks. The equilibrium levitation positions of the two disks are located near the sound pressure node, and the maximum acoustic radiation pressure on their surfaces is less than one percent of the maximum sound pressure.

PACS: 43.25.Uv, 43.20.Ks, 43.25.Qp DOI: 10.1088/0256-307X/36/3/034303

Reflection, refraction, diffraction and scattering of sound beams are the main wave behaviors once an acoustic wave encounters an obstacle. Among these interactions between acoustic waves and interfering objects, scattering of acoustic waves on an object can produce acoustic radiation force. Such an acoustic radiation force can be employed to suspend objects for non-contact transportation and manipulation of objects, which are of fundamental importance for research of many physical or chemical phenomena[1–4] and for applications in biological or engineering fields.[5–8] The typically developed contactless method based on this phenomenon is acoustic levitation. It is a versatile method and has the particular advantage of not being constrained by the electric and magnetic properties of the substance.[9–15]

Tiny droplets,[16,17] small animals,[18] biological cells,[5,6] soap bubbles[14] as well as large polystyrene spheres[12] have been successfully levitated in air by acoustic levitators. However, the object size for levitation by standing-wave field is restricted to the half wavelength, which has becomes a bottleneck for potential applications of such acoustic levitation method.[8,14] Although some efforts have been made to levitating objects beyond the half wavelength limit with ultrasonic waves,[12,14] the enhancement of levitation capability for centimeter sized objects by a single-axis standing-wave levitator still remains the key issue for scientists and engineers due to its promising applications in materials science and industrial assembly fields. Since the investigations have mainly focused on the single wave acoustic levitation,[14,18,19] the dynamic interaction of two confronting ultrasonic waves is still unclear.

In this Letter, we investigate acoustic characteristics of two confronting ultrasonic waves and their levitation capability for disk-shaped objects. Sound pressure fields of two confronting ultrasound beams and a single ultrasonic wave are simulated and compared with different interfering disks. The acoustic radiation force exerting on the disks is measured experimentally and simulated numerically to explore the levitation capability of the two confronting ultrasonic waves.

To have a clear insight into the physical characteristics of the acoustic field yielded by two opposite ultrasound beams, the COMSOL multiphysics software is applied to build the 3D acoustic model. The acoustic field can be expressed by the Helmholtz equation

$$\nabla^2 \Phi + k^2 \Phi = 0, \tag{1}$$

$$p = \rho_0 \frac{\partial \Phi}{\partial t}, \tag{2}$$

where p is the sound pressure, Φ is the velocity potential, k is the wave number, ρ_0 is the density of medium, and v is the medium particle velocity, $\boldsymbol{v} = -\nabla\Phi$. The vibration amplitudes of the top and bottom emitters in calculations are 12 μm and the phases of the two emitters are the same.

The sound pressure distribution is investigated under three operating modes: mode I, two confronting ultrasound beams from emitters A and B; mode Ⅱ, one progressive wave from top emitter A; mode Ⅲ, one progressive wave from bottom emitter B. The diameters of the interfering disks, D, are selected to be 0.25λ, 0.5λ, and λ to clarify the influence of object size on the acoustic field. The thicknesses of the disks, δ, are chosen as 0.02∼0.25λ. Figures 1(a_1)–1(c_1) show the sound pressure distributions with levitation of a disk with diameter of 0.25λ. The acoustic diffraction occurs and the ultrasonic waves travel across the disk. When the diameter of the interfering disk approach λ, the distribution characteristic of acoustic fields changes remarkably related to the three operating modes, as presented in Figs. 1(a_2)–1(c_2). For modes Ⅱ and Ⅲ with a single acoustic wave, the sound pressure between the object and the reflector is quite small compared to that with the levitation

*Supported by the National Natural Science Foundation of China under Grant Nos 51871186 and 51771156.
**Corresponding author. Email: bbwei@nwpu.edu.cn
© 2019 Chinese Physical Society and IOP Publishing Ltd

of a disk with diameter 0.25λ. The diffraction of ultrasonic waves is weakened and the shadow effect is strengthened when the interfering object approaches the wavelength scale. Based on the analyses of acoustic radiation force, mode Ⅱ provides an acoustic radiation force with the same direction of gravity, which can not provide the levitation force for objects. Both modes I and Ⅲ can produce an upward acoustic radiation force. However, the absolute value of the acoustic radiation pressure around the lateral boundary of disk with diameter λ under mode Ⅲ is smaller than that under mode I. This indicates that the lateral constraint under mode I is more favorable for the stable levitation of disks. Hence, we focus on the levitation capability of two confronting ultrasonic waves and the acoustic levitation of centimeter-sized disks under mode I.

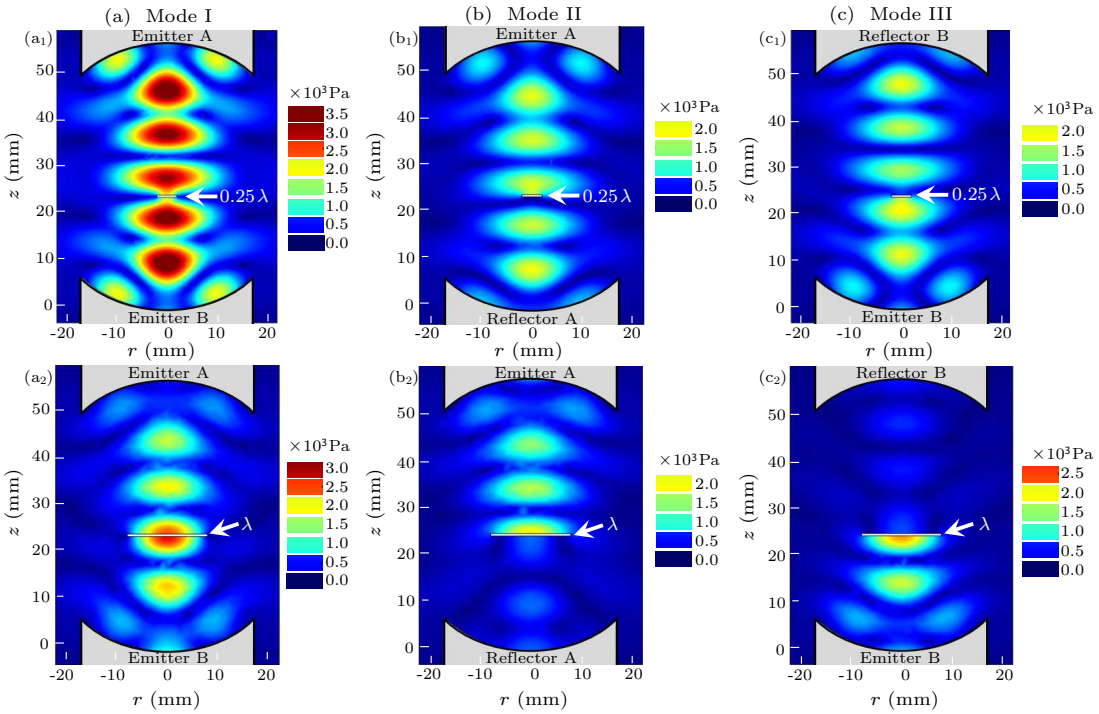

Fig. 1. Sound pressure fields interfered with a thin disk-shaped object with wavelength-scaled diameter under three operating modes: (a) mode I, two confronting ultrasound beams from emitters A and B, (b) mode Ⅱ, one progressive wave from top emitter A, (c) mode Ⅲ, one progressive wave from bottom emitter B; (a_1)–(c_1) a disk with 0.25λ diameter, (a_2)–(c_2) a disk with diameter λ.

A single-axis acoustic levitator based on mode I by employing two opposite transducers arranged with their common axis in the gravitational direction is established. Each transducer has a concave emitting surface and works at a frequency of $f = 21$ kHz, which generates a wavelength of $\lambda = 16$ mm in air at room temperature. The two concave emitters share the same section radius of $d = 17.50$ mm and surface curvature radius of $R = 25$ mm. The vibration amplitudes of emitters A and B are measured by a vibrometer CYS-J200, which are 6 μm and 12 μm, respectively. The interval H between the two emitters is adjusted to be 57.80 mm.

In the experiments, two kinds of centimeter-sized thin disks with radial dimensions up to one wavelength are successfully levitated. One is a clay disk with a diameter of 15.5 mm (0.97λ) and a thickness of 3.5 mm as shown in Fig. 2(a). The weight of the clay disk is 0.0568 g and its density is about 0.101 g/cm^3. Its levitation position z locates at 33.6 mm. The other is an aluminum disk with a diameter of 14.4 mm (0.90λ) and a thickness of 0.35 mm, as presented in Fig. 2(b). The corresponding weight and density of the Al disk are 0.1444 g and 2.414 g/cm^3, respectively. Its levitation position z locates near 33.0 mm.

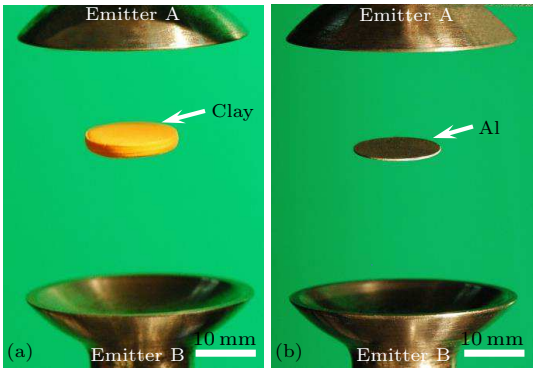

Fig. 2. Acoustic levitation of centimeter-sized thin disks by two opposite ultrasonic beams (mode I): (a) a clay disk with diameter 15.5 mm (0.97λ) and thickness 3.5 mm, and (b) an aluminum disk with diameter 14.4 mm (0.90λ) and thickness 0.35 mm.

A key parameter related to the acoustic levitation as well as acoustic manipulation is the acoustic radiation force F which acts as the levitation force and arises from the scattering of the acoustic waves on the levitated objects.[20,21] The acoustic radiation force F

is measured during the experiments by connecting the object with a slender rod that is fixed to the measuring platform of a digital analytical balance with readability 0.0001 g. When the object is placed in the acoustic field, the acoustic radiation force exerting on the object can be transferred to the compressive force applied on the measuring platform. The acoustic radiation force can thus be measured with an accuracy of 10^{-6} N. A micropositioning slide is used to control the position of the object with a resolution of 0.02 mm.

Figures 3(a)–3(d) show the relationship between the acoustic radiation force F and the vertical position of the disks along the symmetric axis in the z coordinate of the levitator. The largest acoustic radiation force on the clay disk attains 0.073 N. For the Al disk, the largest peak value of the acoustic radiation force reaches 0.066 N. The stable levitation of objects requires the balance between acoustic radiation force and the gravity G, which locates at the intersection points between F and the $F = G$ line. From the enlargement of the acoustic radiation force near the levitation position in Figs. 3(c) and 3(d), it is demonstrated that the disks will fall downward because the acoustic radiation force is smaller than the gravity when the levitated disks move up from the equilibrium levitation position. In contrast, if the disks drop downward, the acoustic radiation force larger than gravity can push them upward. Such a procedure will proceed successively until the objects are stably levitated.[1]

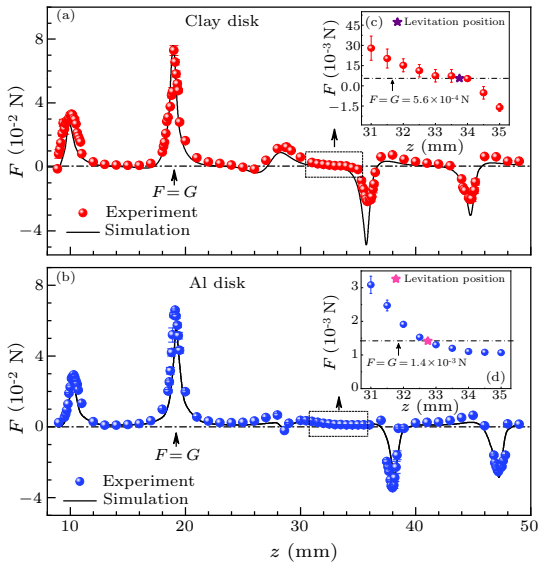

Fig. 3. Acoustic radiation force on interfering disks versus vertical positions (mode I): (a) clay disk and (b) Al disk; (c) and (d) the enlargement of dashed line areas. The red and blue spheres represent the measured data in experiments and the black solid lines indicate the simulation results.

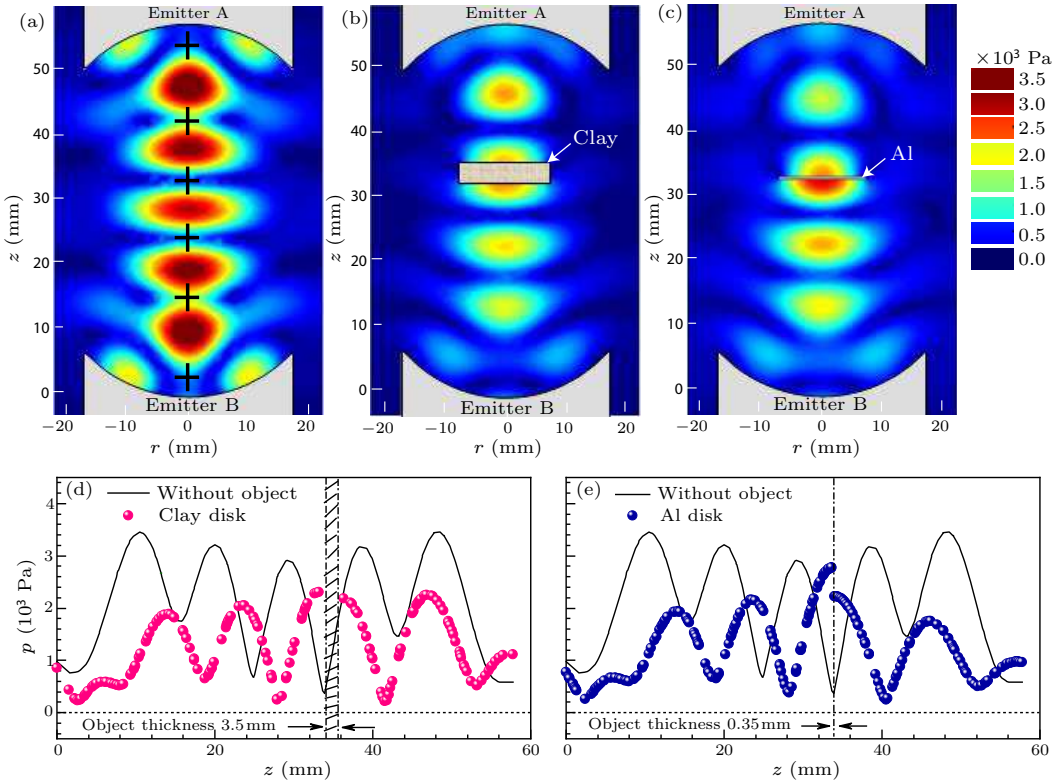

Fig. 4. Distribution profiles of sound pressure fields (mode I): (a) without interfering objects, (b) and (d) interference of the clay disk, (c) and (e) interference of the Al disk. The symbol + in (a) indicates the pressure nodes of the acoustic field without objects; (d) and (e) show the variation of sound pressure without the object and with the interfering of disks along the symmetry axis in the z direction.

Figure 4 presents the simulated sound pressure field with and without the interference of thin disks. Before the interference of the disks, there are six pressure nodes along the symmetric axis between the two emitters as indicated by the symbol +. With the introduction of the disks into the levitator, the sound

pressure field changes significantly. Figures 4(d) and 4(e) show the comparison of sound pressure with the interfering disks and without the levitation of objects along the symmetry axis. It can be seen that the levitation position of the disks locates near the sound pressure node of the original acoustic field which is depicted by the solid lines in Figs. 4(d) and 4(e). The maximum sound pressure appears at the bottom surface of the levitated disks and achieves 2302.05 Pa and 2777.83 Pa with the clay disk and the Al disk, respectively.

King[22] proposed an equation for the acoustic radiation pressure p_a, which results from the second order terms of the sound pressure p and the medium particle velocity v. It can be written as

$$p_a = \frac{1}{2\rho_0 c_0^2}\left\langle p^2\right\rangle - \frac{1}{2}\rho_0\left\langle \boldsymbol{v}^2\right\rangle, \tag{3}$$

where c_0 is the acoustic speed in the medium. The angular brackets denote the time average over one period of acoustic oscillation.

Figure 5 shows the distribution of the acoustic radiation pressure p_a on top and bottom surfaces of disks. There exist both positive pressure and negative pressure on the top and bottom surfaces. The acoustic radiation pressure on the disk surfaces has a tendency to flatten the levitated objects, which is evident in the acoustic levitation of liquid droplets.[4] It should be noted that the maximum positive acoustic radiation pressure is only 18.17 Pa for the clay disk and 25.61 Pa for the Al disk, which is 0.8% and 0.9% of the maximum sound pressure p_m at the disk surfaces.

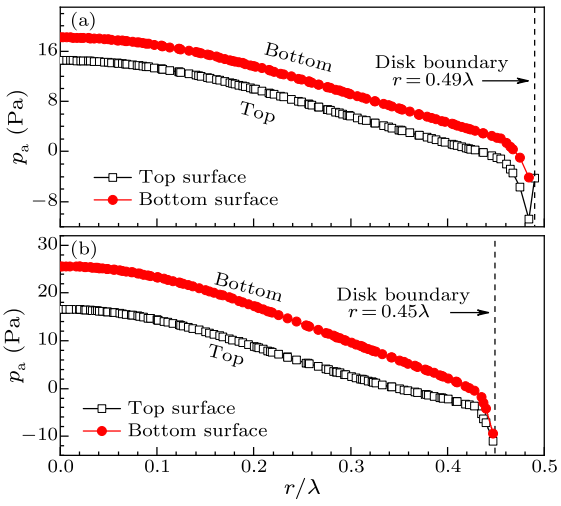

Fig. 5. Calculated acoustic radiation pressures versus radial positions on interfering disk surfaces: (a) clay disk, (b) Al disk.

Although the acoustic radiation pressure is quite small as compared with the sound pressure, it provides the levitation force to levitate the objects.[18] The acoustic radiation force F can be derived from the integral of the acoustic radiation pressure p_a over the entire surface S of the object[20,21]

$$F = -\iint p_a dS. \tag{4}$$

As demonstrated in Figs. 3(a) and 3(b), the calculated acoustic radiation force F depicted with solid lines agrees well with the experimentally measured results.

In summary, we have investigated the acoustic dynamics of two confronting ultrasound beams and their levitation capability for centimeter-sized thin disks. The ultrasonic standing-wave field is strengthened by the superposition of two confronting ultrasound beams when levitating wavelength-scale objects. Two kinds of centimeter-sized disks have been stably levitated in air by two confronting ultrasound waves. One is clay disk with a diameter of 15.5 mm (0.97λ) and the other is the aluminum disk with a diameter of 14.4 mm (0.90λ). The levitation positions of the disks are proved to be stable due to the balance between the levitation force and gravity. Further investigation based on the simulation approach reveals that the acoustic radiation pressure on disk surfaces is much smaller than the sound pressure. These results demonstrate that the levitation capability can be enhanced by employing two opposite ultrasound beams. It may expand the applications of acoustic levitation for larger-sized thin samples in relevant research fields.

References

[1] Baresch D, Thomas J L and Marchiano R 2016 *Phys. Rev. Lett.* **116** 024301
[2] Marzo A et al 2015 *Nat. Commun.* **6** 8661
[3] Bjelobrk N et al 2010 *Appl. Phys. Lett.* **97** 161904
[4] Yan N et al 2011 *Chin. Phys. Lett.* **28** 078101
[5] Foresti D et al 2013 *Proc. Natl. Acad. Sci. USA* **110** 12549
[6] Lam K H et al 2016 *Sci. Rep.* **6** 37554
[7] Vandaele V, Lambert P and Delchambre A 2005 *Opt. Precis. Eng.* **29** 491
[8] Xie W J et al 2004 *Phys. Rev. E* **70** 046611
[9] Ashkin A 1970 *Phys. Rev. Lett.* **24** 156
[10] Geim A K et al 1999 *Nature* **400** 323
[11] Ma X B et al 2013 *Appl. Phys. Lett.* **103** 104101
[12] Andrade M A B, Bernassau A L and Adamowski J C 2016 *Appl. Phys. Lett.* **109** 044101
[13] Zhao S and Wallaschek J 2011 *Arch. Appl. Mech.* **81** 123
[14] Zang D Y et al 2017 *Appl. Phys. Lett.* **110** 121602
[15] Rey C A et al 1988 *Metall. Mater. Trans. A* **19** 2619
[16] Field C R and Scheeline A 2007 *Rev. Sci. Instrum.* **78** 125102
[17] Wu J 1991 *J. Acoust. Soc. Am.* **89** 2140
[18] Xie W J et al 2006 *Appl. Phys. Lett.* **89** 214102
[19] Hu B et al 2017 *Appl. Phys. Lett.* **111** 103504
[20] Bruus H 2012 *Lab Chip* **12** 1014
[21] Mitri F G 2008 *Ann. Phys.* **323** 1604
[22] King V 1934 *Proc. R. Soc. Lond. A* **147** 212